[Article ID] 1003 - 6326(2000)05 - 0666 - 05

Deformation mechanism of tension of 2024 Al alloy at semi-solid state①

DU Zhi-ming(杜之明), LUO Shou-jing(罗守靖), SUN Jia-kuan(孙家宽)
(School of Materials Science and Engineering, Harbin Institute of Technology, Habrin 150001, P.R.China)

[Abstract] The mechanism of the tension and fracture of 2024 Al alloy at semi-solid were theoretically and experimentally investigated, with the isothermal tension of 2024 Al alloy at semi-solid state as an example. Results of theoretical and experimental analysis show that the tensile deformation of 2024 Al alloy at semi-solid state is achieved by the relative sliding of grains and the deformation of liquid membrane under tensile stress. The relative sliding of grains is mainly accommodated by the nucleation and growth of cavities under tensile stress. A cavity will nucleate in the region with the largest hydrostatic stress at first and then grow along preferential grain boundaries, leading to the final fracture of specimen along grain boundaries.

[Key words] semi-solid; tension; 2024 Al; grain relative sliding
[CLC number] TG351 [Document code] A

1 INTRODUCTION

Compared to conventional technologies such as casting and plastic forming, semi-solid metal processing (SSP) is a kind of newly emerging metal processing technology, being highly efficient and low-consuming. So, it is necessary to conduct some theoretical and experimental studies being relevant to SSP[1~7]. Because of the special characteristics of semi-solid metal, its mechanical behaviors and deformation mechanisms will be different from that of solid metal. So, studies on the mechanical behaviors and deformation mechanisms of semi-solid metal will lay a theoretical basis for SSP. Up to now, the mechanical behaviors and deformation mechanisms of the semi-solid compression of alloys and composites have been studied by many researchers, but the deformation mechanisms and damage mode of the semi-solid tension of alloys and composites have rarely been studied[1~8]. There are tensile stresses in the actual semi-solid metal processing technologies, which will lead to the damage of parts. However, it was hard to find references discussing this process. So, the microstructural deformation mechanisms and damage mode of alloys at semi-solid state are investigated in this paper, with 2024 Al alloy as experimental materials and with its semi-solid isothermal tension as example.

2 EXPERIMENTAL

2024 Al alloy was used as experimental materials, the method for determining its melting range was referred to Ref.[7]. The Semisolid raw material used for the semisolid tension test was fabricated by the method of liquidus casting[9]. According to the technique of liquidus casting, the liquid 2024 Al was poured into a steel die at (638 ±2) ℃ and cooled at the ambient temperature. Thus, the semi-solid raw material with non-dendritic microstructure could be produced.

Tensile specimens were cut from the extruded rod after heat treatment along longitudinal direction. Tension tests were conducted on Shimadzu materials testing machine and the tensile temperature was selected as a semi-solid temperature of 575 ℃. Before the tension experiments, the specimen were maintained in furnace at 575 ℃ for about 10 min, and the temperature difference was controlled in the range of ±2 ℃. Tension experiments were conducted in atmosphere without inert gas protection. Tension strain rate in experiments was $0.036\ s^{-1}$. In the process of tension experiments, the deformation force-displacement curve was automatically recorded by testing machine. Because macro necking did not appear in experiments, tensile true stress-true strain curves can be derived by simple calculation, shown as Fig.1. In or-

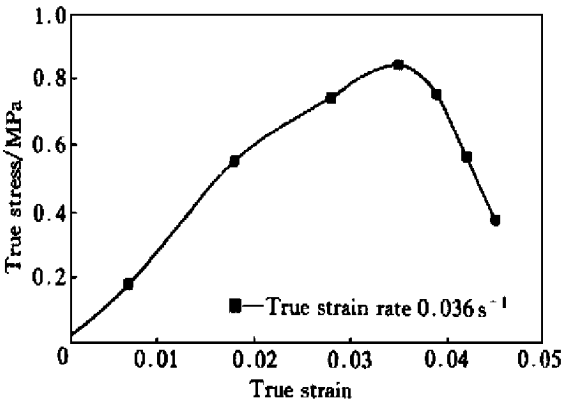

Fig.1 Tensile true stress-true strains curves

① [Received date] 1999 - 08 - 23; [Accepted date] 1999 - 11 - 29

der to observe the microstructure changes of specimen in experiments, the specimen were quickly quenched in cold water immediately after the tension experiments to remain the deformed microstructures. Specimens for the microstructural investigation were prepared by mechanical and chemical polishing process. Electronic probe and SEM were used to observe the microstructure. The fracture surface of tensile specimen was investigated on SEM after the gold-spraying treatment.

3 RESULTS

3.1 Tensile true stress-true strain

It can be seen from Fig.1 that the stress will increase with the increase in the strain at the initial deformation stage, that the stress reaches a peak value when the deformation degree is about 3.7 % and the stress will rapidly decrease with the progress of deformation up to the final fracture of specimen. It also can be seen from Fig.1 that the total strain of specimen is about 4.7 % before the final fracture. However, the ambient elongation of 2024 Al alloy is about 16 %. So, it can be supposed that the liquid phase existing in the grain boundaries will cause the variation of deformation mechanism when specimen is deformed at semi-solid state, leading to the decreasing of the elongation of 2024 Al alloy.

3.2 Microstructure

3.2.1 Liquid volume fraction

The grain boundaries of specimen mainly are liquid phase after its holding at 575 ℃ for about 10 min[7]. Liquid volume fraction can be estimated as about 9.75 % using image method.

3.2.2 After fracture

After the tension experiments, the fracture of specimen can be macrostructurally divided into two kinds: 1) planar fracture surface, perpendicular to tension axis; 2) oblique fracture surface, inclining 45° to tension axis. In order to observe the microstructure change in the process of tensile deformation, two points in the central position of specimen and near the fracture surface were investigated, and the results were shown in Fig.2. In Fig.2, the tension axis is parallel to the longitudinal direction of paper. It can be seen from Fig.2(a) and (b) that there are large cracks in the region near the fracture surface and these cracks mainly consists of two parts: 1) one part existing in the grain boundaries perpendicular to the tension axis, indicated by arrow *A*; 2) another part existing in the grain boundaries inclining a certain angle to the tension axis, indicated by arrow *B*.

In addition, it can be seen from Fig.2 that the grains in the tension specimen rarely undergo plastic deformation when the deformation temperature is 575 ℃ and the strain rate is 0.036 s^{-1}. Fig.3 is SEM

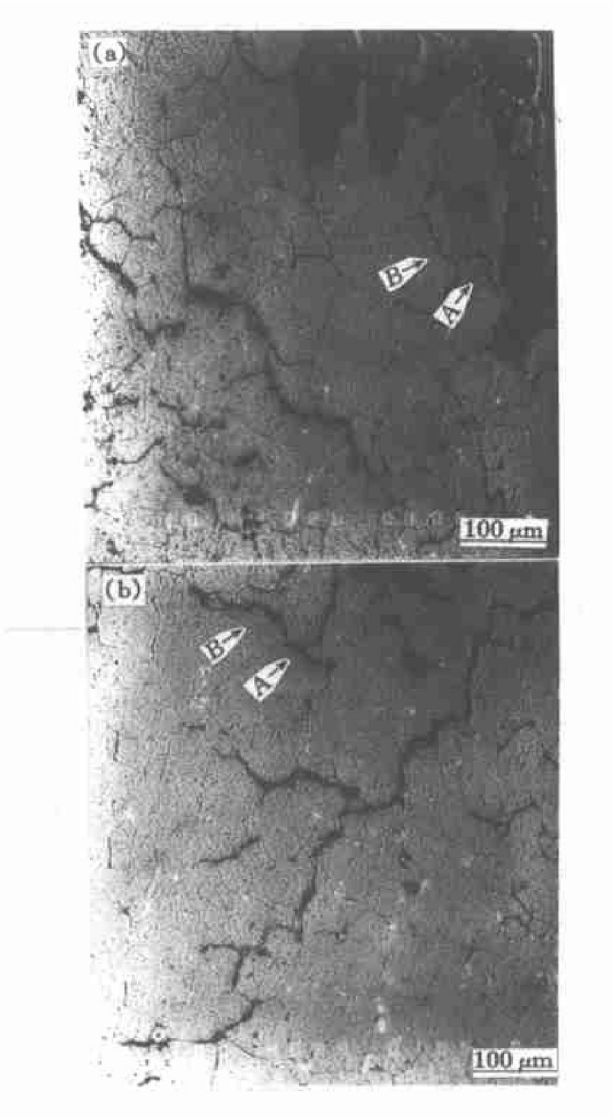

Fig.2 Microstructures of tensile specimen at position near fracture surface
(a) —Oblique fracture surface; (b) —Planar fracture surface

Fig.3 SEM micrograph of fracture surface of tensile specimen

photographs the fracture surface of tensile specimen. It can be obviously found that the tension fracture of 2024 Al alloy at semi-solid is a typical fracture along grain boundaries.

4 DISCUSSION

4.1 Stress state in tensile specimen

Figs.4(a) and (b) show the stress state of different grain boundaries in tensile specimen. It can be seen from Fig.4(a) that the grain boundary *a*-*b* bears the shear stress τ and the tensile stress σ and the grain boundary *c*-*d* do not bear any stress. It can be seen from Fig.4(b) that the stress state of grain boundary *e*-*f* is similar to that of grain boundary *a*-*b* and there is only tensile stress σ on grain boundary *g*-*h*. In addition, a strain will be produced at the interface between solid phase and liquid phase because of the microstructural movement of electrons, inducing an internal stress in liquid phase, because atoms in the liquid phase are not similar to those in the solid phase[10].

According to the requirement of the continuity of the wave function of quantum mechanics, the surface electron density of atoms in the two sides of solid-liquid interface must be equal. However, the surface electron density of atoms in the two sides of solid-liquid interface is not equal. So, in order to meet this requirement, the atoms in the two sides of solid-liquid interface will change their volumes, which causes a volumetric strain in the liquid phase, inducing a internal stress in the liquid phase[10].

Fig.4(c) is a magnified diagram of the grain boundary *a*-*b* in Fig.4(a). It can be understood that the total strain of tensile specimen is mainly composed of two parts: 1) the relative sliding of grains under shear stress, ε_s(shear strain); 2) the deformation of the liquid membrane sandwiched between two solid

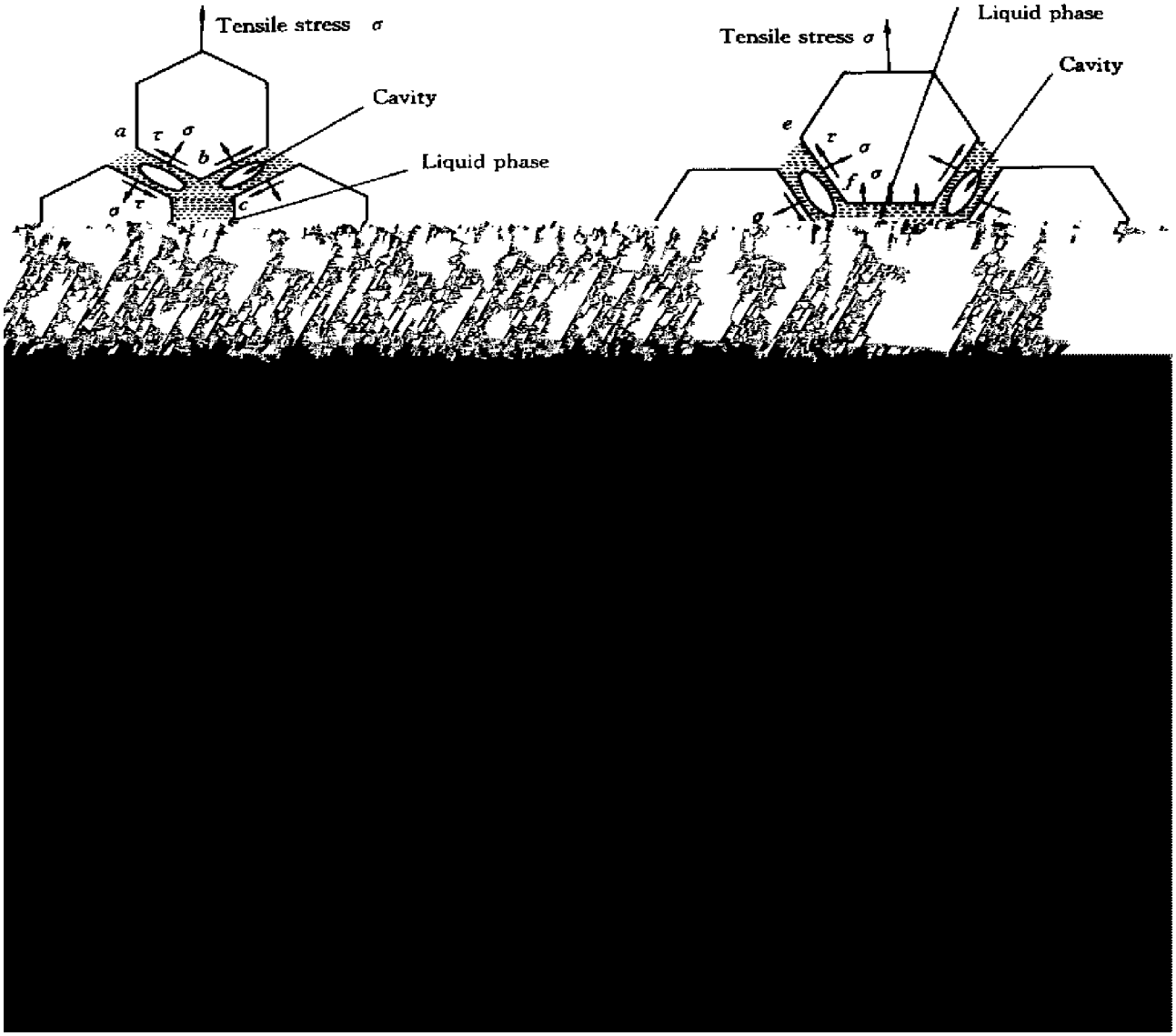

Fig.4 Schematic representation of stress distribution along liquid grain boundaries in tensile specimen
(a) —Position 1; (b) —Position 2; (c) —Magnified diagram of grain boundary *a*-*b*

grains under the tensile stress, ε_t.

4.2 Deformation and fracture mechanisms

It can be supposed that a shear stress and a tensile stress will be produced on grain boundaries when the tensile load is imposed on the tensile specimen, shown as Fig.4. Under the effect of shear stress, the relative sliding of grains will begin to produce a strain. A strain will be produced in the liquid membrane under the effect of tensile stress with increasing the external load, and cavities will greatly nucleate in the liquid phase and grow along certain directions when the tension stress reaches a critical value. At the same time, the externally imposed tensile stress will rapidly decrease, shown as Fig.1.

In addition, the relative sliding of grains mainly is accommodated by the formation of cavities in liquid phase. The formation of cavities consists of two processes, the nucleation and the growth. According to Ref.[6], a cavity will appear in the region with the largest tension stress, namely in the intersection of three grains. It was noted by Marion, Thouless and Evans that the nucleation of cavities in the solid body with liquid grain boundaries needs a critical tension value σ_t and that the nucleation rate of cavities, $\dot{n}$, will rapidly decrease up to zero if the tension stress in liquid phase is lower than this value[6]. Regarding a spherical cavity, if it nucleates in the intersection of three grains, its critical radius r_c and nucleation rate $\dot{n}$ can be expressed by following equation[6]:

$$r_c = \frac{2\gamma}{\sigma} \tag{1}$$

$$\dot{n} = \frac{8kTf_l n_s}{3\eta\Omega^{3/5}}\left(\frac{\gamma}{\sigma}\right)\exp\left(-\frac{16\pi\gamma^3}{3\sigma^2 kT}\right) \tag{2}$$

where f_l is liquid volume fraction, n_s nucleation amount per volume, η the viscosity of liquid phase, γ the surface tension of liquid-gas interface, Ω the volume of atoms or molecules in liquid phase, σ the tension in liquid phase, k Boltzman constant. In addition, it is worth noting that above two equations are based on the hypothesis of homogeneous nucleation. Most of atoms in the liquid phase in the system of this paper are copper atoms. When Cu exists in liquid state, its radius is 0.128 nm, its viscosity is 5.0×10^{-3} Pa·s and its surface tension of liquid-gas interface is 0.38 J/m^2[11]. These parameters were substituted into above two equations to calculate the critical nucleation radius and the nucleation rate. The results of calculation are shown in Fig.5.

It can be seen from Fig.5 that the critical nucleation radius of cavity is about 0.1 ~ 0.2 nm, being equivalent to the radius of copper atoms, which shows that cavities will easily nucleate in the liquid phase under the effect of tension stress. However, it can be seen from Fig.5(a) that it is difficult for a cavity to nucleate in liquid phase if the tension stress is lower than a critical value σ_t(2 500 MPa). It also can be seen from Fig.5(a) that the nucleation of cavities in liquid phase needs the tension stress of 2 500 MPa. Although the external tensile stress is different from the tension stress in the liquid phase, it is surprising to find that the hydrostatic tension stress in the liquid phase is about 2000 times larger than the external tensile stress. So, it can be supposed that there are other causes making possible the nucleation of cavities: 1) the stress concentration due to the irregularity of the size and shape of grains; 2) the effect of inhomogeneous nucleation actually emerging in the liquid phase; 3) the internal stress caused by the change of atoms in the liquid phase under the interface effect[10]. It is possible for a cavity to nucleate in the liquid phase only under the combined effects of above causes. Cavities mainly grow and propagate along liquid grain boundary immediately after they nucleate in the liquid phase. It can be seen from Fig.2 that cavities mainly grow along the grain boundaries perpendicular to the tension axis (indicated by arrow *A*) and the grain boundaries inclining an angle to the tension axis (indicated by arrow *B*) because the largest tensile stress and shear stress exist on these two grain boundaries, but rarely propagate along the grain boundaries parallel to the tension axis. After the cavities grow and converge, the large cracks will appear, leading to the fracture of specimen along grain boundaries.

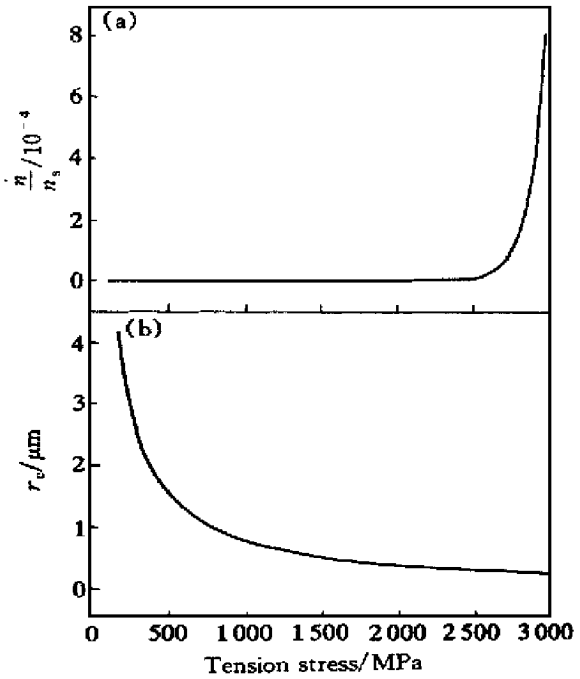

Fig.5 Predictions of critical cavity radii and cavity nucleation rates based on homogeneous nucleation theory
(a) —Cavity nucleation rate; (b) —Critical cavity radii

5 CONCLUSIONS

1) The tensile stress and shear stress will be produced on different grain boundaries after an external tensile load is imposed on the tensile specimen.

2) The total strain mainly consists of two parts: a) the deformation of liquid membrane under the effect of tensile stress; b) the relative sliding of grains under the effect of shear stress.

3) Under the combined effects of the external tensile stress, the stress concentration due to the irregularity of the size and shape of grains, the effect of actually emerging inhomogeneous nucleation and the internal stress caused by the interface effect, a large tension stress will be produced in the liquid phase and the cavities will nucleate in the liquid phase and grow along the preferential grain boundaries, leading to the final fracture of specimen along grain boundaries.

[REFERENCES]

[1] Chen C P and Tsao C Y A. Semisolid deformation of nondendritic structures—1 phenomenological behavior [J]. Acta Mater, 1997, 45(5): 1955 - 1968.

[2] Thanh L N and Suery M. Compressive behavior of partially remelted A356 alloys reinforced with SiC particles [J]. Mater Sci Tech, 1994, 10: 894 - 901.

[3] Martin C L, Favier D and Suery M. Viscoplastic behavior of porous metallic materials saturated with liquid—Part Ⅰ: Constitutive equations [J]. Int J Plast, 1997, 13(3): 215 - 235.

[4] Martin C L, Favier D and Suery M. Viscoplastic behavior of porous metallic materials saturated with liquid—Part Ⅱ: Experimetal identification on a Sn-Pb model alloy [J]. Int J Plast, 1997, 13(3): 215 - 235.

[5] Kang C G and Yoon J H. A finite analysis on the upsetting process of semi-solid aluminum material [J]. J Mater Procs Tech, 1997, 66: 76 - 84.

[6] Vaandrager B L and Pharr G M. Compressive creep of copper containing a liuid bismuth intergranular phase [J]. Acta Met, 1989, 37: 1057 - 1066.

[7] Nieh T G, Wadsworth J and Imai T. A rheological view of high-strain-rate superplasticity in alloys and metal-matrix composites [J]. Scripta Metall Mater, 1992, 26: 703 - 708.

[8] LUO Shou-jing and SUN Jia-kuan. Study on deformation mechanism of compression of 2024Al alloy at semi-solid state [J]. Chinese Science Bulletin, 1999, 44(5): 545 - 549.

[9] LIU Dan. Slurry making by liquidus casting aluminum alloy and the research of technology and theory in semi-solid metal processing [D]. Shenyang: Northeastern University, 1999. 17 - 41.

[10] CHENG Kai-jia and CHENG Shu-yu. Analysis and calculation of internal stress of membrane [J]. Natural Science Progress, 1998, 8(1): 20 - 29.

[11] Wlliam D and Callister, Jr. Materials science and engineering (Third Edition) [M]. John Wiley & Sons, INC, 1994. 45.

[12] Urcola J J and Sellars C M. Effect of changing strain rate on stress-strain behavior during high temperature deformation [J]. Acta Metall, 1987, 35(11): 2637 - 2647.

(Edited by ZHU Zhong-guo)